Key role of organic complexation of iron in sustaining phytoplankton blooms in the Pine Island and Amundsen Polynyas (Southern Ocean)

Thuroczy, Charles-Edouard; Alderkamp, Anne-Carlijn; Laan, Patrick; Gerringa, Loes J. A.; Mills, Matthew M.; Van Dijken, Gert L.; De Baar, Hein J. W.; Arrigo, Kevin R.

Published in:
Deep-Sea research part ii-Topical studies in oceanography

DOI:
10.1016/j.dsr2.2012.03.009

Publication date:
2012

Deep-Sea Research II 71-76 (2012) 49–60

Contents lists available at SciVerse ScienceDirect

Deep-Sea Research II

journal homepage: www.elsevier.com/locate/dsr2

Key role of organic complexation of iron in sustaining phytoplankton blooms in the Pine Island and Amundsen Polynyas (Southern Ocean)

Charles-Edouard Thuróczy [a,*], Anne-Carlijn Alderkamp [b,c], Patrick Laan [a], Loes J.A. Gerringa [a], Matthew M. Mills [c], Gert L. Van Dijken [c], Hein J.W. De Baar [a,b], Kevin R. Arrigo [c]

[a] Royal Netherlands Institute for Sea Research (Royal NIOZ), P.O. Box 59, 1790 AB Den Burg, Texel, The Netherlands
[b] Department of Ocean Ecosystems, University of Groningen, Groningen, The Netherlands
[c] Department of Geophysics, Stanford University, Stanford, CA, USA

ARTICLE INFO

Available online 15 March 2012

Keywords:
Iron
Organic complexation
Ligands
Dissolved
Ratio [L]/[DFe]
Southern Ocean
Amundsen
Pine Island
Polynya
Phytoplankton bloom
Glacier
CLE-AdSV
Dyna LiFe
GEOTRACES
NBP09-01

ABSTRACT

Primary productivity in the Amundsen Sea (Southern Ocean) is among the highest in Antarctica. The summer phytoplankton bloom in 2009 lasted for >70 days in both the Pine Island and Amundsen Polynyas. Such productive blooms require a large supply of nutrients, including the trace metal iron (Fe). The organic complexation of dissolved Fe was investigated in the Amundsen Sea during the spring of 2009 to better understand the potential role of ligands in enhancing the local stock of dissolved Fe. The main sources of Fe and ligands to the Amundsen Sea are thought to be melting sea-ice and the Circumpolar Deep Water (CDW), which is modified (MCDW) on the continental shelf and upwells beneath the coastal glaciers and ice-shelves. Upwelling of relatively warm MCDW is also responsible for the rapid melting of the Pine Island Glacier (PIG) and surrounding ice-shelves, resulting in additional release of Fe into surface waters. At upwelling stations near ice shelves, organic ligands were nearly saturated with Fe, thus enhancing the stock of Fe and its availability to the phytoplankton community. However, ligands had little capacity to buffer additional Fe input from glacial melt. In these coastal upwelling regions, much of the glacial Fe supply is lost due to vertical export of Fe via scavenging and precipitation. Conversely, within the phytoplankton bloom in the nearby coastal polynyas, the uptake of Fe combined with the production of organic matter enhanced the abundance of relatively unsaturated organic ligands capable of stabilizing additional Fe supplied from glacial melt. These unsaturated dissolved organic ligands, combined with the continuous input of Fe (dissolved and particulate) from glacial melt, appear to favor the solubilization of Fe, thus increasing the stock of bioavailable Fe and fueling the phytoplankton bloom.

1. Introduction

The Southern Ocean plays an important role in the export of anthropogenic CO_2 (around 25% of total anthropogenic carbon emission), in part via primary production by phytoplankton (De Baar et al., 1995). Primary productivity is enhanced in polynyas; areas of reduced sea-ice concentration within a more consolidated ice pack (Arrigo et al., 1997; Arrigo and VanDijken, 2003a). Of the dozens of coastal polynyas circling the Antarctic continent, those located in the Amundsen Sea (Fig. 1) exhibit the highest phytoplankton productivity per unit area (Arrigo and VanDijken, 2003b).

Iron (Fe) availability limits algal growth in the high nutrient low chlorophyll (HNLC) regions of the worlds oceans (Martin et al., 1990,1991). The abundance of Fe in seawater is controlled by a balance between Fe input (via sediment resuspension, sea-ice and glacial melt, upwelling, atmospheric deposition, and hydrothermal inputs), stabilization processes via organic complexation that keep Fe in the dissolved phase, and by removal processes like (oxidative) precipitation and adsorptive scavenging (Baker and Croot, 2010; Boye et al., 2001; Croot and Johansson, 2000; Gledhill and Van Den Berg, 1994; Lannuzel et al., 2007, 2008, 2010; Rue and Bruland, 1997; Klunder et al., 2011; Kuma et al., 1996; Nishioka and Takeda, 2000; Nishioka et al., 2001; Thuróczy et al., 2010b, 2011a, 2011b).

Around Antarctica, the two dominant phytoplankton groups include diatoms and the prymnesiophyte *Phaeocystis antarctica*. On the continental shelf, diatoms dominate the phytoplankton community in shallow mixed layers whereas colonial *P. antarctica* dominates in waters with a deep mixed layer (Arrigo et al., 1999, 2002). Because macronutrient concentrations in Southern Ocean waters are so high, distributions of these two taxa are governed

* Corresponding author. Tel.: +31 222 369 459.
E-mail address: Charles-Edouard.Thuroczy@nioz.nl (C.-E. Thuróczy).

0967-0645/$ - see front matter © 2012 Elsevier Ltd. All rights reserved.
http://dx.doi.org/10.1016/j.dsr2.2012.03.009

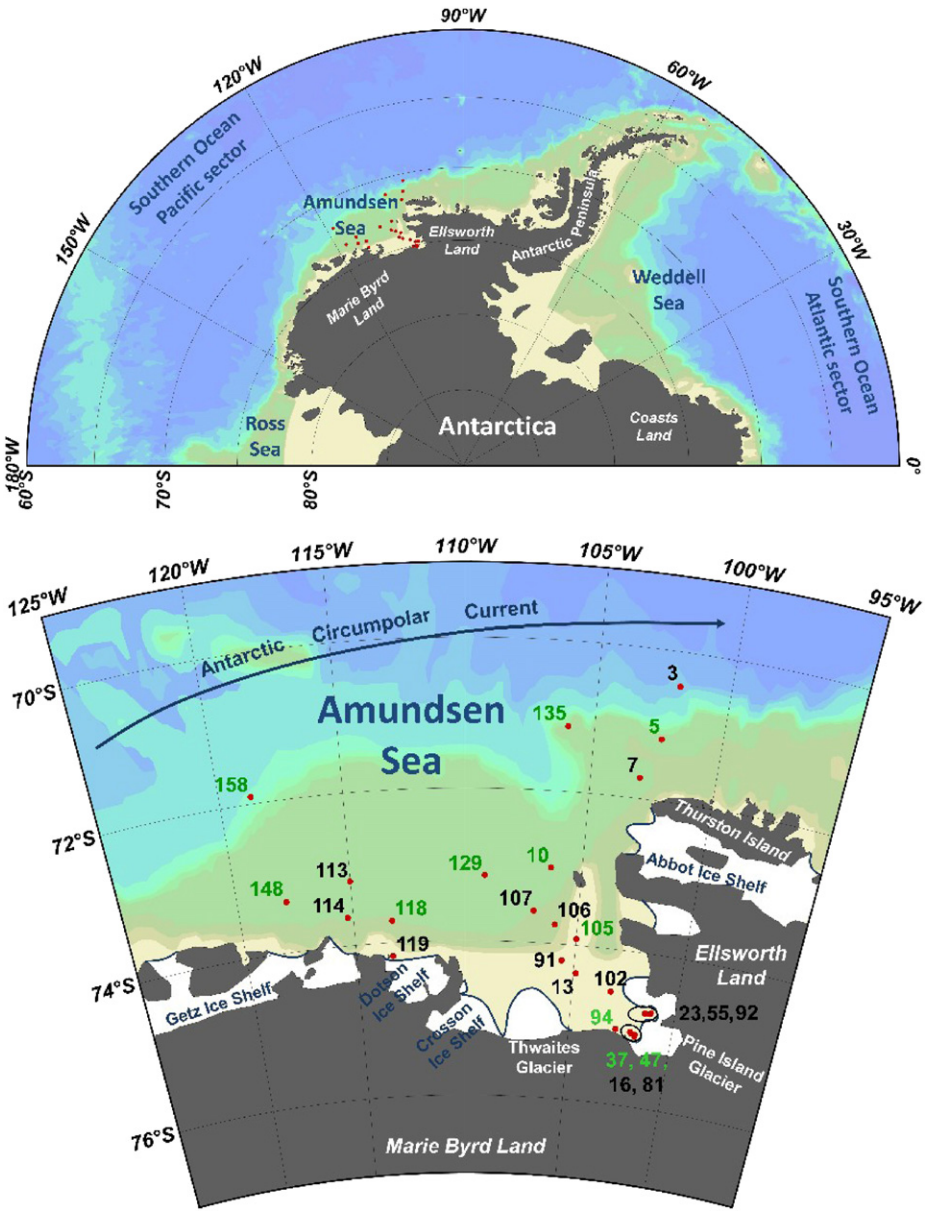

Fig. 1. Map of western Antarctica (A) with the study area enlarged (B). The stations sampled in the Amundsen Sea are shown with numbered red dots (vertical profile=black numbers and surface sampling=green numbers). (For interpretation of the references to color in this figure legend, the reader is referred to the web version of this article.)

by their specific requirements for two main growth-limiting factors, Fe and light (Alderkamp et al., 2012; Buma et al., 1991; Coale et al., 1996; De Baar et al., 1990; 2005; Sunda and Huntsman, 1997; Timmermans et al., 2001;). Diatoms and *P. antarctica* have different nutrient utilization characteristics and support very different higher trophic level communities (Arrigo et al., 1999). In the Southern Ocean, Fe controls the magnitude of annual primary productivity while light determines the taxonomic distribution (Arrigo et al., 2000, 2003; Arrigo and VanDijken, 2003b; Alderkamp et al., 2012). Consequently, increasing sea surface temperature in Antarctica due to global warming could enhance ice melt and subsequent water column stability and alter phytoplankton primary productivity and community structure. Furthermore, the inflow of the warm and Circumpolar Deep Water (CDW, Jacobs and Hellmer, 1996) on the Amundsen Sea shelf drives a rapid melting of the Antarctic ice shelves, in particular the PIG (Jacobs et al., 2011). Melting of the PIG could account for 10% of the present day sea-level rise (Rignot et al., 2008) and is an important and continuous source of Fe to surface waters in Pine Island Bay (PIB) (Gerringa et al., 2012).

The Amundsen Sea is delimited by the Abbot Ice Shelf in the North-East (Fig. 1) and the Crosson, Dotson, and Getz Ice Shelves on the west side of PIB. The Amundsen Sea has a large continental shelf area, is about 250–400 m deep and has deep canyons (up to 1600 m depth, Nistche et al., 2007). PIB is surrounded by two main glaciers: the Thwaites Glacier on the western side and the PIG to the south. The Antarctic Circumpolar Current (ACC, Fig. 1) flows eastwards around the Antarctic continent and injects relatively warm (~2 °C) and saline (34.0–34.5) CDW (Giulivi and Jacobs, 1997) onto the Amundsen Sea continental shelves. This CDW then flows towards the continent and upwells underneath the PIG and the Getz and Dotson Ice Shelves. The CDW inflow is partly responsible for the rapid melting (Jacobs and Hellmer, 1996) of the ice shelves of the Amundsen Sea, as well as of the Thwaites and Pine Island glaciers (Jenkins et al., 2010). These waters also harbor two large and productive polynyas, the

Pine Island Polynya (PIP) and the Amundsen Polynya (AP) (Arrigo and VanDijken, 2003b).

The organic complexation of Fe in the dissolved fraction (<0.2 μm) was studied in the Amundsen Sea during the cruise NBP09-01 onboard the US Research Vessel *Nathaniel B. Palmer* from 5 January until 28 February 2009. The research goal was to gain insight into the role of the ligands in increasing the potential solubility of Fe by buffering Fe input from upwelling of MCDW and glacial melt, and thus indirectly enhancing its bio-availability to the phytoplankton. This work is part of the DynaLiFe project (Shedding a **dyna**mic **li**ght on **Fe** limitation in the Southern Ocean) which studied *in situ* phytoplankton primary productivity and taxonomic composition in relation to Fe limitation and dynamic changes in irradiance (Alderkamp et al., 2012). Details on the hydrography and Fe distributions in the Amundsen Sea are described in Gerringa et al. (2012). The phytoplankton characteristics and nutrient distribution are described in Alderkamp et al. (2012).

2. Materials and methods

2.1. Sampling and filtration

Samples were taken in the upper 300 m of the water column (at 10, 25, 50, 100, 200, 300 m) using modified Teflon coated GO-FLO samplers (General Oceanics, Inc.) attached to a non-metal 6 mm diameter wire. These were closed using PVC messengers. The GO-FLO samplers were brought one by one to a trace metal clean container and linked to a tubing extension for sub-sampling under a clean laminar flow bench. Samples were filtered (0.2 μm pore size, Sartorius Sartobran-300) using slight N_2 overpressure. All samples were collected in previously acid-cleaned (3 steps cleaning procedure with detergent solution, 6 M HCl and 3 M nitric acid in 60ºC hot bath; detailed by Middag et al., 2009) LDPE bottles after 5 rinses with the sample itself. Samples for the analysis of the Fe speciation were stored at 0°C if analysis could be performed within 2 day; otherwise they were immediately frozen at −20°C.

Organic complexation of Fe was determined at 26 stations from 12 January to 15 February (Fig. 1, Table 1), 15 of which included multiple samples from vertical profiles (St. 3, 7, 13, 16, 23, 55, 81, 91, 92, 102, 106, 107, 113, 114 and 119) and 11 stations (St. 5, 10, 37, 47, 94, 105, 118, 129, 135, 148, 158) from which only one sample was taken from surface waters (10 m depth) in conjunction with experiments studying the effects of light and ligands additions on phytoplankton physiology. These experiments are described by Mills et al. (2012).

2.2. Iron analyses

Shipboard analysis of dissolved Fe was done using an in-line Flow Injection Analysis system with chemiluminescence as a detection method (De Baar et al., 2008a,b; De Jong et al., 1998) and is described in detail by Gerringa et al. (2012). In addition, unfiltered samples (19 profiles and 8 surface stations) were taken and acidified to pH=1.8 for at least 6 months of dissolution before being analyzed in the same way as for DFe in the home laboratory. Standard deviations of the duplicate or triplicate measurements of one sample were lower than 5%. Accuracy and reproducibility were checked by regularly measuring two SAFe reference standard samples. The results, S1 0.078 ± 0.012 nM DFe ($N=10$) and D2 0.942 ± 0.043 nM ($N=13$), were well within the community consensus values (S1: 0.097 ± 0.043 nM DFe ($N=140$), D2: 0.91 ± 0.17 nM ($N=168$), Johnson et al., 2007).

2.3. Organic complexation of Fe: sample treatment, voltammetric procedure and calculations

Organic complexation of Fe was determined by Competing Ligand Exchange–Adsorptive Stripping Voltammetry (CLE-AdSV) using 2-(2-Thiazolylazo)-p-cresol (TAC) as a competing ligand (Croot and Johansson, 2000). The equipment, voltammetric procedures, sample and chemical preparations are described by Thuróczy et al. (2011a).

Table 1
Stations sampled for this study, with number, sampling date, coordinates, location, bottom depth and sea-ice conditions (*0=sea-ice free; 1/2=partly covered; 1=completely covered). PIP: Pine Island Polynya; PIG: Pine Island Glacier; AP: Amundsen Polynya; DIS: Dotson Ice Shelf. At the profile stations samples were taken at several depths as listed in Table 2. Sub-surface (Sub-S) samples were taken at 10–15 m depth.

Station	Date	Lat. (°S)	Long. (°W)	Location		Bottom depth (m)	Sea-ice condition*	Sampling type
3	12-Jan	70.46	101.93	Open Ocean		3292	0	Profile
5	13-Jan	71.19	102.38	Slope	Eastern part	1095	½	Sub-S
7	14-Jan	71.73	103.04	Shelf		763	1	Profile
10	15-Jan	73.01	106.35	PIP		697	0	Sub-S
13	16-Jan	74.36	104.89	PIP		1294	0	Profile
16	17-Jan	75.07	101.77	PIG	Southern part	948	0	Profile
23	18-Jan	74.77	101.43	PIG	Northern part	739	0	300 m
37	20-Jan	75.04	102.01	near PIG	Southern part	921	0	Sub-S
47	22-Jan	75.06	101.95	near PIG	Southern part	805	0	Sub-S
55	23-Jan	74.77	101.30	PIG	Northern part	677	0	Profile
81	25-Jan	75.09	101.78	PIG	Southern part	940	0	Profile
91	27-Jan	74.21	105.60	PIP		1028	0	Profile
92	28-Jan	74.77	101.20	PIG	Northern part	670	0	Profile
94	28-Jan	75.02	102.74	near PIG	Southern part	805	0	Sub-S
102	30-Jan	74.55	103.18	PIP		1091	0	Profile
105	31-Jan	73.92	105.00	PIP		318	0	Sub-S
106	31-Jan	73.75	106.02	PIP		873	0	Profile
107	1-Feb	73.58	107.00	PIP		970	0	Profile
113	3-Jan	73.16	115.02	AP		763	0	Profile
114	3-Jan	73.63	115.25	AP		923	0	Profile
118	4-Feb	73.71	113.29	AP		837	0	Sub-S
119	4-Jan	74.17	113.34	DIS		588	0	Profile
129	7-Feb	73.14	109.18	PIP		460	0	Sub-S
135	10-Feb	71.13	106.03	Slope	Eastern part	518	1	Sub-S
148	13-Feb	73.34	117.86	AP		365	0	Sub-S
158	15-Feb	71.90	118.71	Slope	Western part	1118	½	Sub-S

The increments of Fe concentrations used in the titration were 0, 0.2, 0.4, 0.6, 0.8, 1.0, 1.2, 1.5, 2, 2.5, 3, 4, 6, 8 and 10 nM.

Total ligand concentrations [Lt] (in equivalents of nanomolar Fe, Eq of nM Fe), the conditional stability constants K′ (mol^{-1}) of the natural organic ligands, and their respective standard deviations of the fit of the data to the Langmuir model (Gledhill and Van Den Berg, 1994) were calculated using non-linear regression (Gerringa et al., 1995). Underlying assumptions are that all Fe(III) species are at equilibrium, all binding sites between Fe and the unknown ligand are equal, and the binding is reversible. The sensitivity (S) was corrected for the influence of ligand sites not yet saturated, as explained by Turoczy and Sherwood (1997) and Hudson et al. (2003). The correction was done by an algebraic solution of the equilibrium equations, in which S is determined together with Lt and K′. The equations for the calculation of Fe speciation are described in Thuróczy et al. (2010a and 2011b). Finally the excess ligand (L′) concentrations were calculated as [L′]=[Lt]−[DFe].

2.4. Chlorophyll-a analysis

Chlorophyll a (Chl *a*) was quantified using standard JGOFS procedures (JGOFS, 1996). Chl *a* samples (0.05–1 L) were filtered at ambient seawater temperature under low vacuum pressure. Filters were extracted in 5 mL 90% acetone in the dark at 4 °C for 20 h. The extracted fluorescence was read before and after acidification using a Turner Designs Model 10-AU fluorometer.

3. Results

3.1. Dissolved iron and total dissolvable iron.

Concentrations of dissolved Fe (DFe) in this study ranged between 0.042 nM (=42 pM) at the chlorophyll maximum (St. 3) and 1.31 nM at the surface near the PIG (St. 55) (Table 2, Fig. 2).

At open ocean stations, Fe concentrations were low with a nutrient-like profile (Fig. 2), being depleted at the surface (0.04–0.06 nM at St. 3 and 0.03 nM at St. 160) and higher at 300 m depth (0.23 nM at St. 3 and 0.16 nM at St. 160). The concentration of DFe measured at 300 m depth at these stations resembled the calculated mean DFe concentration of 0.28 nM ($\pm$0.06, n=20) measured in the CDW in the Pacific section presented by Klunder and De Baar (submitted). DFe concentrations were higher near the shelf at St. 3. Surface DFe concentrations (10 m depth) were relatively high (0.4 nM) at St. 7 where sea-ice was abundant (Table 2, Fig. 2) compared to St. 3 where no ice was present (Fig. 2). In the PIP, sub-surface minima in DFe concentrations were measured just below the Chl *a* maximum (20–25 m depth) below which [DFe] increased with depth to 0.2–0.6 nM (Fig. 2). Stations at or near the PIG, where no phytoplankton was present, had higher DFe concentrations (0.3–1.3 nM) that were relatively constant with depth (Fig. 2). At the Dotson Ice Shelf (St. 119), DFe increased with depth from 0.14 nM at 25 m depth to 0.54 nM at 300 m depth (Table 2, Fig. 2).

The concentrations of total dissolvable Fe (TDFe) are reported in detail by Gerringa et al. (2012). At the open ocean stations (St. 160) [TDFe] were low (0.31–4.31 nM TDFe) as showed by Gerringa et al. (2012). At the ice covered stations, [TDFe] was relatively constant with depth, varying between 0.2 and 6.1 nM for both surface and deeper samples. The concentrations of TDFe measured in the Pine PIP were relatively constant in the upper 100 m (between 1.4 and 5.9 nM) and higher in deeper waters. At St.102, [TDFe] varied between 7.5 and 14.3 nM Fe in the upper 100 m but was much higher in deeper waters (34.4 nM TDFe). Near PIG, [TDFe] averaged 32.6 nM (St. 16), whereas St. 55 on the northern end of the PIG had an average TDFe concentration of 8.1 nM. Station 119, near the Dotson Ice Shelf, had a maximum [TDFe] at 300 m depth, with a value of 105.8 nM.

3.2. Ligand characteristics

The concentrations and depth distributions of dissolved organic ligands (Lt) and excess ligands (L′) varied markedly between the different environments sampled. At St. 3 (open ocean) and St. 7 (sea-ice covered) Lt and L′ concentrations were similar to each other, except in the upper 50 m, where [Lt] and [L′] were lower at St. 7 than at St. 3 (Figs. 2 and 3). Within the bloom of the PIP (St. 13, 91, 106 and 107), values of [Lt] were highest at the surface ($>$0.6 Eq of nM Fe) and lowest at a depth of 200 m (Table 2, Fig. 2). Concentrations of L′ within the center of the bloom in the PIP (St. 13 and 91) were highest at the surface (0.56 and 0.88 Eq of nM Fe, respectively) and decreased with depth to 0.12 and 0.04 Eq of nM Fe at 300 m, respectively (Table 2, Fig. 3). At stations sampled a few days later (4–5 days) during the bloom (St. 106 and 107, Fig. 3), [L′] increased below a minimum at 50 m depth, from 0.41 to 0.58 Eq of nM Fe at St. 106 and from 0.32 to 0.64 Eq of nM Fe at St. 107. At the southernmost station of the PIP (St. 102), the highest [Lt] was measured at 200 m depth (0.9 Eq of nM Fe). Near the PIG (St. 16, 55, 81 and 92), [Lt] and [L′] were relatively high ($>$0.8 Eq of nM Fe, Figs. 2 and 3) and variable at the surface, with the highest [Lt] from this study measured at St. 55 (1.64 Eq of nM Fe). [Lt] and [L′] were relatively constant below 100 m, but differed between stations. These lateral and temporal differences in [Lt] and [L′] presumably reflected the variable currents and hydrography in the vicinity of the PIG (Gerringa et al., 2012). In the Amundsen Polynya, [Lt] and [L′] showed no consistent trend with depth (Figs. 2 and 3). At the Dotson Ice Shelf (Figs. 2 and 3), [Lt] and [L′] were similar to values near the PIG, with a surface maximum for both [Lt] and [L′] at 20 m, and a uniform distribution at greater depths.

The Lt/DFe ratio highlights the saturation state of the organic ligands (Thuróczy et al., 2010b, 2011a, 2011b); this ratio is consistently >1 in open ocean water samples. A low ratio (close to 1) corresponds to ligands relatively saturated with Fe and indicates a low capacity of the ligands to bind and buffer additional Fe input. A relatively high ratio (e.g. >5) indicates that the ligand pool is unsaturated with Fe and can buffer additional Fe input. A high Lt/DFe ratio therefore increases potential Fe solubility and maintains Fe in the dissolved phase.

The Lt/DFe ratios measured here showed consistent trends with depth and location. At the open ocean (St. 3) and sea-ice covered (St. 7) stations, the ratio (1-2) was minimal at the surface and higher (4-13) at a depth of $\sim$50 m. In contrast, both the PIP and AP exhibited the highest Lt/DFe ratio at the surface (5-15), which decreased with depth to <4 at 300 m (Figs. 3 and 5). At the stations influenced by the upwelling of MCDW from under the PIG, the ratios were very low (<2.5) and approximately constant with depth. The ratios from the deepest samples (300 m depth) were always lower than samples from surface waters in the polynyas.

Lastly, the conditional stability constant (K') of the ligands varied between $10^{23.04}$ at St. 114 (in the AP) at a depth of 50 m (Table 2) and $10^{21.14}$ at St. 16 (close to the PIG) at 300 m. At St. 3 and 7, K' was maximal at the surface ($10^{22.5}$) and minimal at 50 m depth ($10^{21.5}$). The K' values were maximal up to 100 m depth at St. 106 and 107 ($>10^{22.4}$) in the PIP as compared to stations sampled a few days earlier in the same area (St. 13 and 91). At the PIG stations, K' ranged from $10^{21.14}$ to $10^{22.96}$, varying with depth, location, and between days (i.e. St. 16 and 81 were taken almost at the same location).

Table 2
Concentrations of dissolved Fe ([DFe] in nM ± standard deviations, S.D.) and Fe-binding ligand characteristics of all samples. Total ligand and excess ligand concentrations ([Lt] and [L′], respectively are in Eq of nM Fe (± standard deviations, S.D.). Conditional stability constants K' are in mol^{-1} with standard deviations; S is the sensitivity of the titration measurement (slope of the straight part of the titration curve, in amp mol^{-1}).

Location	Station number	Depth (m)	[DFe] (nM)	S.D.	[Lt] (Eq of nM Fe)	S.D.	log K' (mol^{-1})	S.D.	Sensitivity	S.D.	[L′] (Eq of nM Fe)	log alpha L	pFe (M)	Lt/Fe
Open ocean	**3**	10	0.110	0.011	0.314	0.066	22.49	0.42	1.53	0.01	0.20	12.80	22.75	2.84
		25	0.064	0.007	0.461	0.104	21.78	0.38	2.19	0.03	0.40	12.38	22.57	7.17
		50	0.042	0.031	0.545	0.142	21.40	0.20	2.18	0.04	0.50	12.10	22.48	12.96
		100	0.075	0.024	0.569	0.119	21.63	0.19	1.54	0.03	0.49	12.33	22.45	7.55
		200	0.177	0.013	0.531	0.114	21.95	0.36	2.07	0.04	0.35	12.49	22.25	2.99
		300	0.228	0.010	0.494	0.123	22.07	0.30	1.55	0.03	0.27	12.50	22.14	2.16
Continental slope	**5**	10–15	0.220	N.D.	0.522	0.270	21.44	0.32	2.18	0.05	0.30	11.92	21.58	2.37
	135	10–15	0.126	N.D.	0.853	0.039	22.31	0.12	1.94	0.01	0.73	13.18	23.08	6.79
	158	10–15	0.087	N.D.	0.908	0.051	22.16	0.11	1.88	0.02	0.82	13.07	23.13	10.44
Shelf	**7**	10	0.395	0.000	0.453	0.042	22.41	0.27	1.94	0.021	0.06	12.18	21.58	1.15
		25	0.083	0.017	0.316	0.056	22.34	0.31	1.34	0.015	0.23	12.70	22.78	3.80
		50	0.082	0.031	0.220	0.148	21.59	0.41	1.87	0.04	0.14	11.73	21.82	2.69
		100	0.128	0.016	0.698	0.103	21.83	0.15	1.73	0.037	0.57	12.59	22.48	5.44
		200	0.186	0.010	0.524	0.103	22.01	0.38	2.06	0.036	0.34	12.54	22.27	2.81
		300	0.271	0.001	0.413	0.101	22.37	0.38	1.49	0.030	0.14	12.52	22.09	1.52
PIP	**10**	10–15	0.098	N.D.	0.396	0.186	21.50	0.32	1.41	0.02	0.30	11.98	21.99	4.06
	13	10	0.099	0.004	0.658	0.117	21.56	0.16	1.79	0.03	0.56	12.30	22.31	6.62
		25	0.092	0.005	0.684	0.119	21.61	0.16	1.52	0.02	0.59	12.38	22.42	7.47
		50	0.078	0.013	0.394	0.065	22.12	0.36	1.85	0.02	0.32	12.62	22.73	5.06
		100	0.115	0.009	0.413	0.071	22.27	0.60	1.41	0.02	0.30	12.75	22.69	3.61
		200	0.112	0.014	0.246	0.042	22.58	0.36	1.73	0.01	0.13	12.70	22.66	2.20
		300	0.607	0.004	0.725	0.076	22.08	0.21	1.50	0.02	0.12	12.15	21.37	1.19
	91	10	0.111	0.004	0.986	0.278	21.28	0.21	1.57	0.04	0.88	12.22	22.17	8.89
		25	0.102	0.012	0.498	0.076	21.98	0.25	1.90	0.03	0.40	12.57	22.56	4.88
		50	0.119	0.011	0.731	0.284	21.33	0.34	1.84	0.05	0.61	12.11	22.04	6.15
		100	0.176	0.018	0.496	0.080	21.93	0.29	1.49	0.02	0.32	12.44	22.19	2.83
		200	0.298	0.008	0.447	0.087	21.99	0.37	1.44	0.02	0.15	12.17	21.69	1.50
		300	0.460	0.005	0.499	0.087	21.79	0.25	1.73	0.02	0.04	11.38	20.72	1.08
	102	10	0.172	0.006	0.611	0.114	21.76	0.25	1.90	0.03	0.44	12.40	22.16	3.55
		20	0.107	0.001	0.387	0.144	21.62	0.60	1.39	0.02	0.28	12.07	22.04	3.61
		40	0.153	0.005	0.514	0.063	22.56	0.55	1.45	0.02	0.36	13.12	22.94	3.37
		100	0.225	0.004	0.733	0.069	22.48	0.23	1.86	0.05	0.51	13.18	22.83	3.26
		200	0.304	0.006	0.895	0.079	22.11	0.14	1.48	0.03	0.59	12.88	22.40	2.94
		300	0.318	0.005	0.588	0.046	22.37	0.19	1.39	0.02	0.27	12.80	22.30	1.85
	105	10–15	0.095	0.003	0.222	0.262	21.34	0.42	1.28	0.04	0.13	11.44	21.47	2.35
	106	25	0.073	0.003	0.578	0.061	22.41	0.37	1.66	0.02	0.50	13.11	23.25	7.89
		50	0.096	0.002	0.511	0.053	22.64	0.83	1.48	0.01	0.41	13.26	23.27	5.30
		100	0.143	0.005	0.573	0.049	22.79	0.79	1.68	0.02	0.43	13.42	23.26	4.01
		300	0.252	0.007	0.831	0.091	22.03	0.19	1.51	0.02	0.58	12.79	22.39	3.29
	107	25	0.044	0.010	0.656	0.049	22.85	0.60	1.44	0.01	0.61	13.63	23.99	14.75
		50	0.053	0.005	0.372	0.034	22.49	0.30	1.44	0.01	0.32	12.99	23.26	6.95
		100	0.068	0.002	0.591	0.039	22.42	0.18	1.43	0.01	0.52	13.14	23.31	8.64
		300	0.457	0.015	1.096	0.072	22.20	0.15	1.91	0.02	0.64	13.01	22.35	2.40
	129	10–15	0.081	N.D.	0.912	0.092	21.90	0.15	1.54	0.02	0.83	12.82	22.92	11.31
PIG (Northern part)	**23**	300	0.446	0.007	0.883	0.135	21.54	0.14	1.56	0.03	0.44	12.18	21.53	1.98
	55	10	1.313	0.014	1.643	0.328	21.59	0.13	2.17	0.13	0.33	12.11	20.99	1.25
		25	0.479	0.003	0.632	0.117	21.80	0.26	1.72	0.02	0.15	11.99	21.31	1.32
		50	0.589	0.035	0.678	0.067	22.41	0.36	1.46	0.02	0.09	12.36	21.59	1.15
		100	0.283	0.014	0.537	0.190	21.66	0.64	1.21	0.03	0.25	12.06	21.61	1.90
		200	0.482	0.022	0.854	0.151	21.58	0.18	1.63	0.03	0.37	12.15	21.47	1.77

Table 2 (*continued*)

Location	Station number	Depth (m)	[DFe] (nM)	S.D.	[Lt] (Eq of nM Fe)	S.D.	log K' (mol^{-1})	S.D.	Sensitivity	S.D.	[L′] (Eq of nM Fe)	log alpha L	pFe (M)	Lt/Fe
		300	0.643	0.080	0.724	0.097	22.04	0.27	1.88	0.03	0.08	11.95	21.14	1.13
	92	50	0.610	0.019	1.149	0.147	21.96	0.22	1.21	0.02	0.54	12.69	21.91	1.88
		100	0.609	0.011	0.988	0.083	22.48	0.21	1.46	0.04	0.38	13.06	22.27	1.62
		200	0.416	0.005	0.883	0.103	22.43	0.24	1.27	0.05	0.47	13.10	22.48	2.12
		300	0.584	0.002	0.971	0.050	22.75	0.24	1.58	0.02	0.39	13.34	22.57	1.66
PIG (Southern part)	**16**	10	0.498	0.009	0.842	0.206	21.57	0.32	1.86	0.04	0.34	12.11	21.41	1.69
		25	0.449	0.007	0.653	0.144	21.94	0.35	1.67	0.05	0.20	12.25	21.60	1.46
		50	0.455	0.007	0.591	0.224	21.41	0.38	1.57	0.03	0.14	11.54	20.89	1.30
		100	0.451	0.008	0.823	0.204	21.34	0.19	1.79	0.04	0.37	11.91	21.26	1.82
		300	0.485	0.001	0.96	0.36	21.14	0.24	2.04	0.05	0.47	11.82	21.13	1.97
	37	10-15	0.236	0.045	0.640	0.096	22.12	0.41	1.55	0.02	0.40	12.73	22.35	2.71
	47	10-15	0.247	N.D.	0.729	0.148	21.60	0.21	1.89	0.04	0.48	12.28	21.89	2.95
	81	50	0.416	0.001	0.907	0.060	22.36	0.17	1.54	1.50	0.49	13.05	22.43	2.18
		100	0.466	0.017	0.960	0.048	22.96	0.43	1.82	1.78	0.49	13.65	22.98	2.06
		200	0.434	0.008	1.032	0.055	22.33	0.14	1.62	1.59	0.60	13.11	22.47	2.38
		300	0.525	0.006	1.148	0.078	22.18	0.15	2.01	1.95	0.62	12.98	22.26	2.19
	94	10-15	0.094	0.001	0.620	0.173	21.53	0.23	1.79	0.05	0.53	12.25	22.28	6.61
AP	**113**	20	0.045	0.005	0.650	0.032	22.60	0.20	1.67	0.01	0.61	13.39	23.74	14.56
		40	0.088	0.010	0.651	0.071	22.39	0.33	1.26	0.02	0.56	13.14	23.20	7.39
		100	0.159	0.001	0.995	0.092	21.95	0.13	1.35	0.02	0.84	12.87	22.67	6.28
		300	0.210	0.010	0.509	0.091	21.98	0.31	1.37	0.02	0.30	12.46	22.14	2.42
	114	25	0.102	N.D.	0.554	0.071	22.26	0.37	1.67	0.02	0.45	12.91	22.91	5.45
		50	0.078	0.018	0.613	0.049	23.04	0.36	1.60	0.01	0.53	13.77	23.88	7.89
		100	0.161	0.016	0.647	0.041	22.63	0.30	1.36	0.01	0.49	13.31	23.10	4.01
		300	0.238	0.009	1.038	0.065	22.19	0.15	1.45	0.01	0.80	13.09	22.72	4.37
	118	10-15	0.109	N.D.	1.127	0.174	21.84	0.22	1.74	0.04	1.02	12.84	22.81	10.36
	148	10-15	0.077	N.D.	1.048	0.076	22.02	0.13	1.22	0.01	0.97	13.00	23.12	13.68
DIS	**119**	25	0.136	0.038	1.455	0.209	21.78	0.11	1.55	0.07	1.32	12.90	22.76	10.68
		50	0.303	0.011	0.791	0.056	22.14	0.12	1.92	0.02	0.49	12.82	22.34	2.61
		100	0.362	0.016	1.097	0.105	21.87	0.11	1.61	0.03	0.74	12.74	22.18	3.04
		300	0.545	0.000	0.871	0.053	22.54	0.16	1.87	0.02	0.33	13.05	22.32	1.60

Excess ligand: [L']=[Lt]−[DFe].
Organic alpha: $\alpha_{organic}=[L'] \times K'$.
pFe$=-\log\{[DFe]/(\alpha_{inorganic}+\alpha_{organic})\}$ (M).
Ratio Lt/Fe: [Lt]/[DFe].

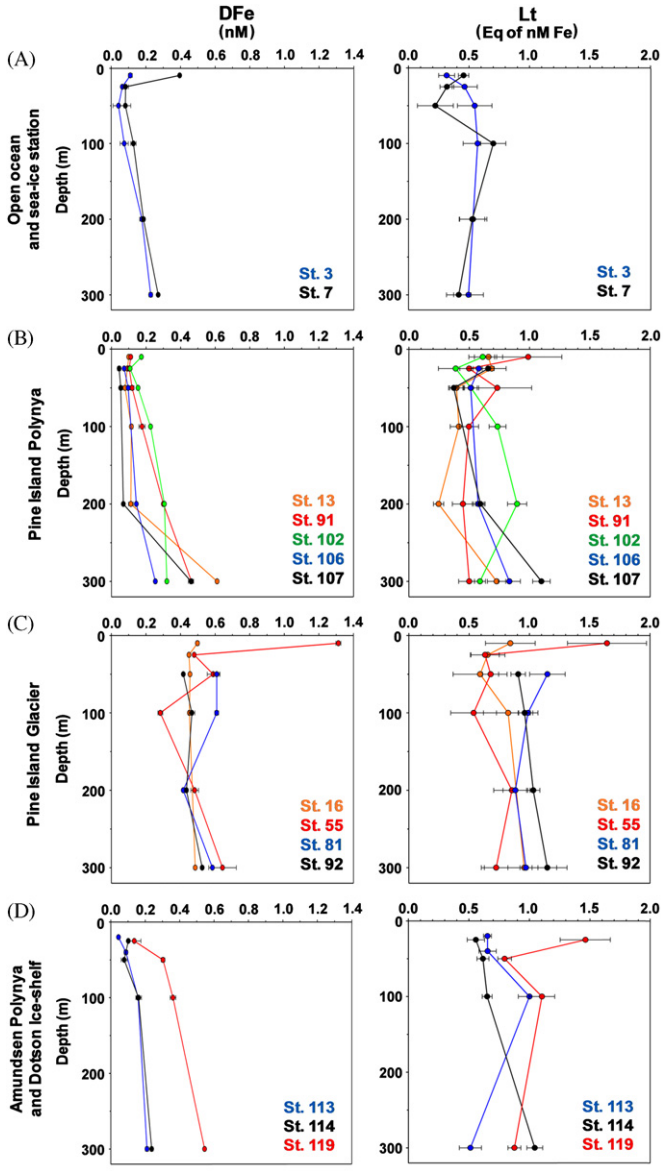

Fig. 2. Vertical distribution of dissolved Fe (DFe, left panels) and dissolved organic ligands (Lt, right panels) in the upper 300 m of the water column. (A) Open ocean (St. 3) and sea-ice station (St.7); (B) Pine Island Polynya (St. 13, 91, 102, 106, 107); (C) Pine Island Glacier (St. 16, 55, 81, 92); (D) Amundsen polynya (St. 113 and 114) and Dotson Ice shelf (St. 119)

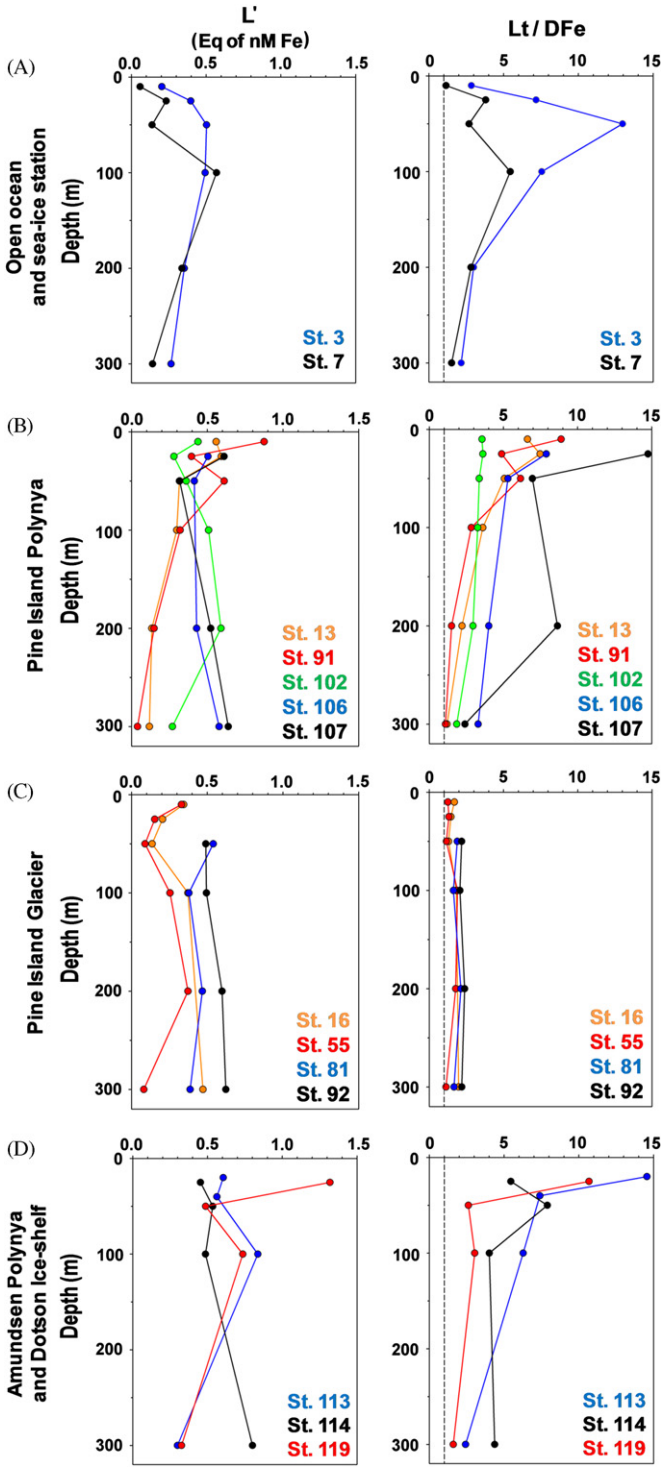

Fig. 3. Vertical distribution of excess ligand (L', left panels) and the Lt/DFe ratio (right panels) in the upper 300 m of the water column. The dashed line marks the exact saturation of the ligands at the Lt/DFe ratio=1. (A) Open ocean (St. 3) and sea-ice station (St. 7); (B) Pine Island Polynya (St. 13, 91, 102, 106, 107); (C) Pine Island Glacier (St.16, 55, 81, 92); (D) Amundsen polynya (St. 113 and 114) and Dotson Ice shelf (St. 119)

4. Discussion

In 2009, the austral summer phytoplankton blooms persisted for more than 70 days in the Pine Island and Amundsen Polynyas (Arrigo et al., 2012). Such productive blooms require a large supply of major nutrients (nitrate, phosphate and silicate) but also of the essential trace nutrient Fe. In the Amundsen Sea, the presence of Fe-complexing organic ligands, combined with the various sources of Fe (Gerringa et al., 2012), played an important role in keeping Fe in solution and enhancing its availability to the phytoplankton bloom.

4.1. Upwelling of CDW on the continental shelf and underneath the ice shelves

In the Amundsen Sea, warm and salty CDW flows over the continental shelf towards the Antarctic continent at a depth of 200–500 m. While in transit, the MCDW is enriched in Fe as explained by Gerringa et al. (2012) who concluded that the increase of DFe and TDFe in the inflowing MCDW from 0.2 to 0.4 nM DFe and from 4 to 7–14 nM TDFe is due to Fe fluxes from the sediments. A further increase to 0.57 nM DFe and 22.4–38 nM TDFe was observed near the glaciers. In the present study, only the upper 300 m were sampled, but because of the MCDW

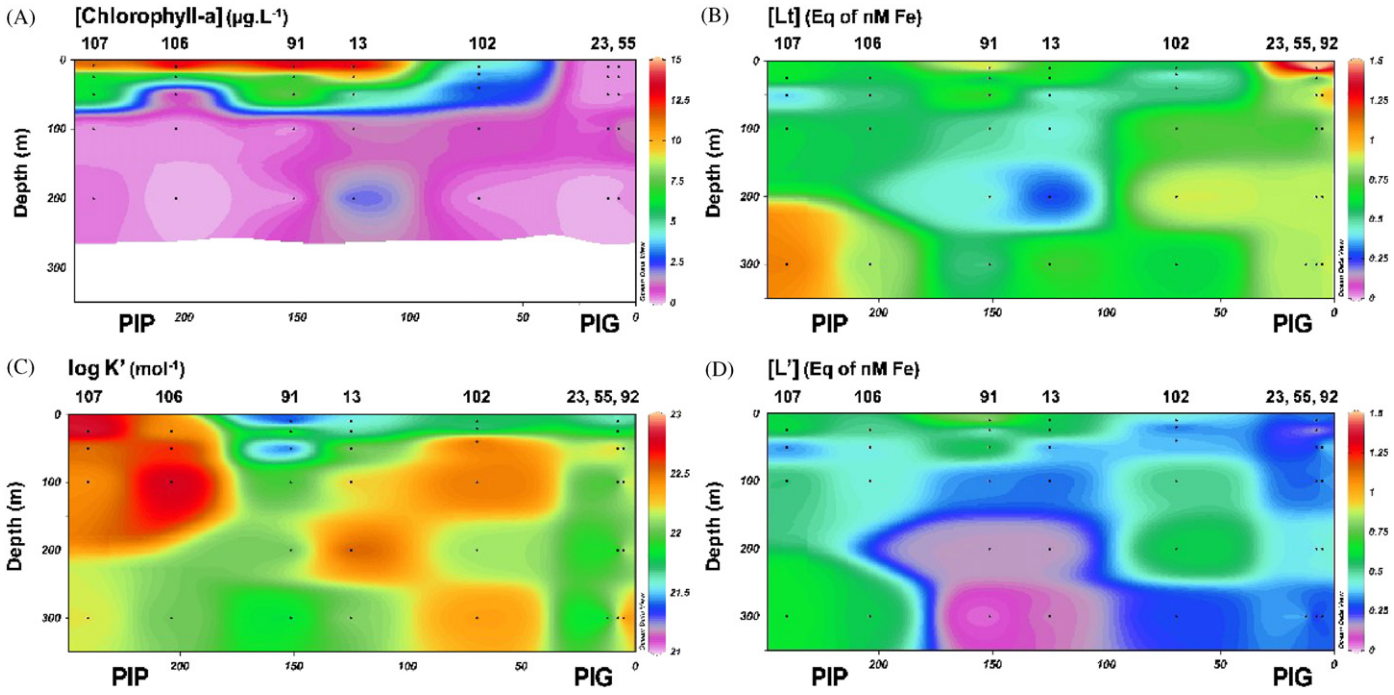

Fig. 4. Vertical sections from the Pine Island Polynya (PIP) to the Pine Island Glacier (PIG) of (**A**) chlorophyll-*a* concentration, (**B**) Lt concentration, (**C**) log *K'*, and (**D**) L' concentration. The lower horizontal axis represents the distance (km) from the Pine Island Glacier; station numbers are shown in the upper axis. Made using Ocean Data View.

upwelling in the Amundsen Sea, higher ligand concentrations were observed in surface waters at both the PIG ([Lt] > 1 Eq of nM Fe, Fig. 4B) and the Dotson Ice Shelf stations. While flowing along the continental shelf, the CDW is likely enriched in ligands by both fluxes from the sediments and settling organic matter produced at the sea surface that is degraded and transformed while sinking towards the sea floor. The enrichment of ligand concentrations by sediments has been observed previously in deep waters of the Kerguelen Plateau (Gerringa et al., 2008) and on Arctic shelves (Thuróczy et al., 2011b). In the Ross Sea, Fitzwater et al. (2000) attributed high concentrations of particulate Fe to fluxes from the sediments from the continental shelf. Therefore, the high ligand concentrations measured at the glacier stations are most likely due to fluxes from the sediments that enriched the CDW. The ligands transported there are dissolved molecules but are also probably under colloidal forms. These colloidal ligands originating from transformation and degradation of organic matter in deep waters may be misinterpreted as organic ligands, because colloidal-Fe may not react significantly with the added ligand TAC during the equilibration time during the measurement, as suggested by Croot and Johansson (2000). Our results suggest that part of the dissolved Fe is transported from the glaciers towards the Polynyas under complexed forms and that the presence of cannot be excluded. Further investigation on size fractionation would bring valuable information.

Furthermore, this warm MCDW drives basal melting of the floating glaciers and ice-shelves that releases in seawater material (sediment, nano-particles) containing iron (Raiswell et al., 2006; Raiswell, 2011). Together with the land erosion engendered by glacier and ice shelf motion, terrigenous material is released into the seawater. Terrigenous materials quickly release metals that are weakly bound to their matrix once in contact with seawater (within 2 h, as seen for Co and Zn, Thuróczy et al., 2010a). These metals may dissolve in the surrounding melted water, hence contributing to the elevated concentrations of DFe (> 0.4 nM, Table 2 and Fig. 2) and [TDFe] (10–35 nM Fe at the PIG ice shelf stations; Gerringa et al., 2012). However, large refractory particles likely sink before dissolution as already found by Croot et al. (2004 and 2007) who showed that a significant amount of iron (dissolved and particulate) supply to the upper waters is rapidly removed by aggregation and sinking. It is generally assumed that 90% of these particles will sink out of surface waters in the vicinity of the glacier (De Baar and de Jong, 2001; Raiswell et al., 2006). In opposition, finer particles may be transported away from the glacier and dissolve over the time, thereby releasing DFe into the seawater. Land erosion is likely to be a large source of Fe but not of ligands (no organic matter input) whereas the input of organic ligands is most likely due to the enrichment of the CDW by the sediments and by sinking organic matter produced by the phytoplankton blooms and its degradation and transformation while sinking out of the water column. Both inputs of Fe by the glacier and of organic ligands by the MCDW upwelling lead to saturation of the ligands in the vicinity of the glacier, as confirmed by the Lt/DFe ratios that shows ligands near saturation at the ice shelf stations of both the PIG and the Dotson Ice shelf.

4.2. Phytoplankton bloom

Within the blooms of the PIP and AP, phytoplankton uptake resulted in low concentrations of DFe (Table 2, Figs. 2 and 4A) (Alderkamp et al., 2012; Gerringa et al., 2012). On the section from the PIP to the PIG (Figs. 4A and 5), the phytoplankton bloom was accompanied by very high Lt/DFe ratios (> 5, Figs. 3 and 5) due to both DFe uptake and ligand production from organic matter generated by the bloom. The ligands, being relatively unsaturated with Fe, form a potential for solubilizing Fe from external sources via organic complexation. Phytoplankton and other microorganisms during the spring and summer generate huge quantities of organic matter during growth and subsequent senescence (Pusceddu et al., 1999). The residence time of bioavailable Fe may be increased by the presence of exopolysaccharides (EPS, Hassler et al., 2011a, 2011b) released by microorganisms in the upper waters that act as Fe-binding ligand, thereby extending the phytoplankton blooms. Degradation and

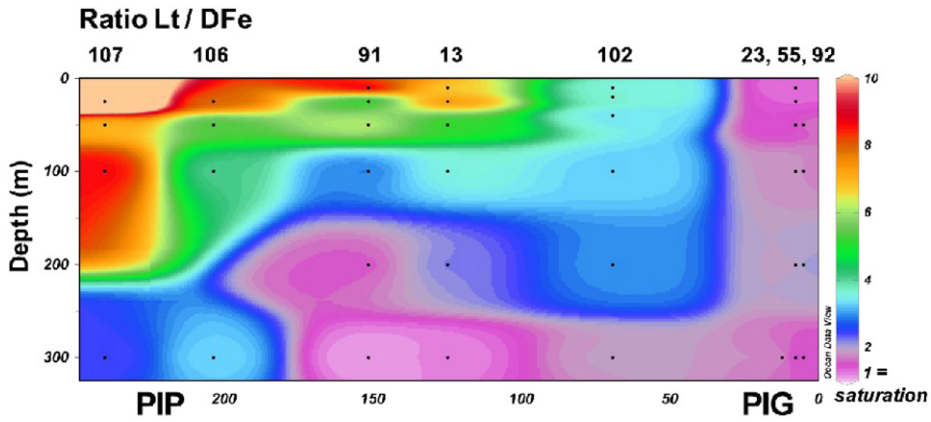

Fig. 5. Vertical section of the Lt/DFe ratio from the Pine Island Polynya (PIP) to the Pine Island Glacier (PIG). The lower horizontal axis represents the distance (km) from the Pine Island Glacier; station numbers are shown in the upper axis. Made using Ocean Data View.

remineralization of organic matter aid in the regeneration of ligands (Gerringa et al., 2006), hence participating in the regeneration of Fe from senescent phytoplankton in surface waters, but also in enriching deep waters with organic matter and thus organic ligands.

At stations 13 and 91, the K' of the ligands was relatively low (<21.6, Table 2, Fig. 4C) when compared to stations in the PIP that were sampled several days later during the bloom (>22.4, St. 106 and 107). The increase of K' over time may indicate that the availability of Fe decreased locally, which is consistent with a lower maximum photochemical efficiency of photosystem II (F_v/F_m) in surface waters of these stations when compared to other stations in the PIP (Alderkamp et al., 2012). Fe-stress may have resulted in production of Fe-binding siderophores by heterotrophic bacteria in order to enhance Fe availability (Barbeau et al., 2001; Butler, 2005; Maldonado et al., 2005). This is consistent with observations by Rue and Bruland (1997) and Cullen et al. (2006) who demonstrated the existence of relatively strong ligands in the presence of phytoplankton.

Sarthou et al. (2008) suggested that approximately 50% of the Fe used by phytoplankton could be regenerated at the surface, thus generating a local stock of Fe that would be available to the microbial community. The presence of unsaturated organic ligands may promote the stabilization of this regenerated Fe by keeping it in solution and preventing aggregation and sinking. The regenerated Fe can be immediately utilized by plankton or become trapped along with organic matter when sea-ice forms later in the season (Kepkay, 1994; Thomas et al., 2001; Lannuzel et al., 2007,2008; Ackermann et al., 1994; Reimnitz et al., 1993; Sherwood, 2000; Smedsrud, 1998). This material, together with organic matter produced by the microbial community living within the sea-ice, are released the following season when the sea-ice melts (Lannuzel et al., 2010) and act as a source of dissolved ligands (Aguilar-Islas et al., 2008; Calace et al., 2001; Nichols et al., 2005; Pankowski and McMinn, 2008). Iron released from melting sea-ice may be pivotal for initiating the spring phytoplankton bloom, thanks to the presence of ligands that solubilize Fe.

4.3. Role of the ligands in solubilizing Fe from melting glaciers

At stations located near the PIG and Dotson Ice Shelf, the concentrations of iron were high and ranged between 0.4 and 0.8 nM for DFe, reaching 1.31 nM DFe in the surface layer at St. 55(Table 2 and Fig. 2) and from 8 to 106 nM for TDFe (Gerringa et al., 2012). Because of these high concentrations of DFe and Lt, the ensuing Lt/DFe ratio indicated that ligands were near saturation (ratio of <2, hence low L′ concentrations); consequently, removal of non-ligand-bound Fe via scavenging may increase. Furthermore, at those stations close to the glaciers, the high TDFe concentrations observed by Gerringa et al. (2012), together with the presence of saturated organic ligands, could facilitate vertical export of Fe (dissolved and particulate) via scavenging, as suggested by Sedwick et al. (2000) for the Ross Sea. This high potential for scavenging of Fe in the vicinity of the PIG likely contributes to elevated particulate Fe concentrations in the deep waters.

On the transect from the PIG to the PIP, the concentrations of TDFe from unfiltered samples still were relatively high as far as 62.5 km away from the PIG with concentrations corresponding to a third of the concentrations found at the source, as described by Gerringa et al. (2012). However it is difficult to assess the effect of lateral turbulent flux on TDFe, therefore this distance represents an indication of the effect and strength of the glacier source on the elevation of TDFe concentrations in this area. This suggests either that particulate Fe can be transported laterally for relatively long distances, as has been seen over the Arctic continental slope (Thuróczy et al., 2011b), or that particulate Fe near the glacier is mainly inorganic while the particulate Fe within the bloom is mostly organic (contained in phytoplankton cells). In the upper 50 m of the water column between the PIG and PIB, organic ligands became increasingly desaturated (ratio Lt/DFe increased, Figs. 3 and 5). On the same transect, there was a clear decrease in both [DFe] and [TDFe] (Gerringa et al., 2012), as well as in [Lt], but an increase in [L′] (Figs. 3 and 4). These trends fit with the hypothesis that part of the Fe present in the particulate phase may be solubilized due to the presence of unsaturated dissolved organic ligands. However, the role of the kinetic exchanges between dissolved and particulate phases still needs to be investigated in order to explain these observations. In addition, solubilization of Fe in surface waters may have been enhanced due to photoreduction (Kuma et al., 1992; Kuma et al., 1995; Powell and Wilson-Finelli, 2003).

During the winter season when there is little biological uptake of Fe, the ligand pool in the PIP most likely becomes fully saturated (very low Lt/DFe ratios) due to the continuous input of Fe from glacial melt driven by upwelling of MCDW. Part of the Fe input from glacial sources during the winter would be unable to remain in solution and would precipitate when [L'] falls below the solubility product of the Fe oxy-(hydr)oxides. This probably results in the export of non-complexed Fe towards the bottom and represents a plausible mechanism for enrichment of Fe in deep waters (the CDW) in the vicinity of the glaciers during the winter. Part of the exported Fe may undergo dissolution,

remineralization, and/or transformation as colloidal Fe and be upwelled again after descending into the MCDW flow.

5. Summary

During the austral summer 2009 in the Amundsen Sea, the presence of unsaturated dissolved organic ligands, combined with the continuous input of Fe (dissolved and particulate) from glacial melt, proved to be an important process enhancing Fe availability for phytoplankton, thus contributing to the long-lasting bloom.

The inflow of CDW onto the Amundsen continental shelf was enriched in both Fe and ligands from the sediments. Further Fe and ligand enrichment took place when warmer CDW upwelled beneath the PIG, causing basal melt of the glacier and releasing terrigenous material containing Fe into the seawater. The melting of the PIG driven by the upwelling of this modified CDW is likely an important source of both Fe and ligands. High concentrations of organic ligands (despite the low [L′] at the PIG stations) increased the potential Fe solubility, thus maintaining a sufficient stock of dissolved Fe, increasing its bioavailability to the phytoplankton. In the Ross Sea Polynya and probably others, low Fe concentrations limit phytoplankton growth at the end of the bloom (Arrigo et al., 2000, 2003); however, in the Amundsen Sea, a prolonged phytoplankton bloom is facilitated through the continuous input of ligands and Fe in modified CDW that upwells and melts the glaciers and ice shelves that surround the local polynyas.

Near the ice shelf, organic ligands were nearly saturated with Fe, as evidenced by the low Lt/DFe ratio (<2), corresponding to low excess ligand concentrations. This shows that most of the additional Fe added during glacial melting may be removed via scavenging and/or precipitation, leading to an enrichment of Fe of the deep waters. Additionally, the massive phytoplankton blooms produce huge quantities of organic matter that is remineralized as it sinks out of the water column, thereby enriching the CDW that flows along the continental shelf and eventually upwells from beneath the glaciers and ice shelves. The uptake of Fe by the phytoplankton bloom, caused the desaturation of the organic ligands at the surface. The production of organic ligands (organic matter and probably siderophores) enlarges even the magnitude of this desaturation. This likely favors the solubilization of Fe from the particulate phase and may play a role in the horizontal transport of Fe from the glacier northwards towards the polynyas.

During the winter, when light is too low to support phytoplankton growth, Fe is not consumed and organic ligands become saturated with Fe. This most likely halts the solubilization of Fe from the particulate phase, enhancing the loss of Fe via scavenging. During spring, nearly saturated ligands near the glaciers become fully saturated, leaving no free space for binding new Fe input, leading to its loss via precipitation. The consequence of this Fe export from the surface to the bottom is winter enrichment of Fe in the CDW inflow, generating a loop pathway as CDW is upwelled beneath the ice shelves.

Acknowledgments

The authors are most grateful to the Captain and crew of R.V. *Nathaniel B. Palmer*, as well as to Stanley Jacobs, chief scientist during the NBP09-01 cruise. National Science Foundation DynaLiFe grant to KRA (ANT-0732535) as part of the International Polar Year and by the Netherlands Organization for Scientific Research (NWO), Netherlands AntArctic Programme (NAAP Grant 851.20.041).

References

Ackermann, N.L., Shen, H.T., Sanders, B., 1994. Experimental studies of sediment enrichment of arctic ice covers due to wave action and frazil entrainment. J. Geophys. Res. 99 (C4), 7761–7770.

Aguilar-Islas, A.M., Rember, R.D., Mordy, C.W., Wu, J., 2008. Sea ice-derived dissolved iron and its potential influence on the spring algal bloom in the Bering Sea. Geophys. Res. Lett. 35, L24601.

Alderkamp, A.-C., Mills, M.M., van Dijken, G.L., Laan, P., Thuróczy, C.-E., Gerringa, L.J.A., de Baar, H.J.W., Payne, C., Tortell, P., Visser, R.J.W., Buma, A.,.G.J., Arrigo, K.R., 2012. Iron from melting glaciers fuels phytoplankton blooms in Amundsen Sea (Southern Ocean); phytoplankton characteristics and productivity. Deep-Sea Res. II 71–76, 32–48.

Alderkamp, A.-C., Kulk, G., Buma, A.G.J., Visser, R.J.W., Van˜Dijken, G.L., Mills, M.M., Arrigo, K.R., 2012. The effect of iron limitation on the photophysiology of *Phaeocystis antarctica* (Prymnesiophyceae) and *Fragilariopsis cylindrus* (Baccillariophyceae) under dynamic irradiance. J. Phycol 48 (1), 45–59.

Arrigo, K.R., Worthen, D.L., Lizotte, M.P., Dixon, P., Dieckmann, G., 1997. Primary production in Antarctic Sea Ice. Science 276 (5311), 394–397, http://dx.doi.org/:10.1126/science.276.5311.394.

Arrigo, K.R., Robinson, D.H., Worthen, D.L., Dunbar, R.B., DiTullio, G.R., VanWoert, M., Lizotte, M.P., 1999. Phytoplankton community structure and the drawdown of nutrients and CO_2 in the Southern Ocean. Science 283, 365–367.

Arrigo, K.R., DiTullio, G.R., Dunbar, R.B., Lizotte, M.P., Robinson, D.H., VanWoert, M., Worthen, D.L., 2000. Phytoplankton taxonomic variability and nutrient utilization and primary production in the Ross Sea. J. Geophys. Res. 105 (C4), 8827–8846.

Arrigo, K.R., Dunbar, R.B., Robinson, D.H., Lizotte, M.P., 2002. Taxon-specific differences in C/P and N/P drawdown for phytoplankton in the Ross Sea, Antarctica. Geophys. Res. Lett. 29 (20)http://dx.doi.org/:10.1029/2002GL015277.

Arrigo, K.R., VanDijken, G.L., 2003a. Impact of iceberg C-19 on Ross Sea primary production. Geophys. Res. Lett. 30 (16), 1836, http://dx.doi.org/:10.1029/2003GL017721.

Arrigo, K.R., VanDijken, G.L., 2003b. Phytoplankton dynamics within 37 Antarctic coastal polynyas systems. J. Geophys. Res. 108 (C8), 3271, http://dx.doi.org/:10.1029/2002JC001739.

Arrigo, K.R., Worthen, D.L., Robinson, D.H., 2003. A coupled ocean-ecosystem model of the Ross Sea: 2. Iron regulation of phytoplankton taxonomic variability and primary production. J. Geophys. Res. 108 (C7). 3231, 10.1029/2001JC000856.

Arrigo, K.R., Lowry, K., Van Dijken, G., 2012. Annual changes in sea ice and phytoplankton in polynyas of the Amundsen Sea, Antarctica. Deep-Sea Res. II 71–76, 5–15.

De Baar, H.J.W., Buma, A.G.J., Nolting, R.F., Cadée, G.C., Jacques, G., Tréguer, P.J., 1990. On iron limitation of the Southern Ocean: experimental observations in the Weddell and Scotia Seas. Mar. Ecol. Prog. Ser. 65 (2), 105–122.

De Baar, H.J.W., de Jong, J.T.M., Bakker, D.C.E., Löscher, B.M., Veth, C., Bathmann, U., Smetacek, V., 1995. Importance of iron for plankton blooms and carbon dioxide drawdown in the Southern Ocean. Nature 373 (6513), 412–415.

De Baar, H.J.W., de Jong, J.T.M., 2001. Distributions, sources and sinks of iron in seawater. In: Turner, D.R., Hunter, K.A. (Eds.), The Biogeochemistry of Iron in Seawater. Wiley, Chichester, UK, pp. 123–254. Chap. 5.

De Baar, H.J.W., Boyd, P.W., Coale, K.H., Landry, M.R., Tsuda, A., Assmy, P., Bakker, D.C.E., Bozec, Y., Barber, R.T., Brzezinski, M.A., Buesseler, K.O., Boye, M., Croot, P.L., Gervais, F., Gorbunov, M.Y., Harrison, P.J., Hiscock, W.T., Laan, P., Lancelot, C., Law, C.S., Levasseur, M., Marchetti, A., Millero, F.J., Nishioka, J., Nojiri, Y., VanOijen, T., Riebesell, U., Rijkenberg, M.J.A., Saito, H., Takeda, S., Timmermans, K.R., Veldhuis, M.J.W., Waite, A.M., Wong, C.S., 2005. Synthesis of iron fertilization experiments: from the iron age in the age of enlightenment. J. Geophys. Res. 110, C09S16.

De Baar, H.J.W., Gerringa, L.J.A., Laan, P., Timmermans, K.R., 2008a. Efficiency of carbon removal per added iron in ocean iron fertilization. Mar. Ecol. Prog. Ser. 364, 269–282.

De Baar, H.J.W., Timmermans, K.R., Laan, P., de Porto, H.H., Ober, S., Blom, J.J., Bakker, M.C., Schilling, J., Sarthou, G., Smit, M.G., Klunder, M., 2008b. Titan: a new facility for ultra-clean sampling of trace elements and isotopes in the deep oceans in the international Geotraces program. Mar. Chem. 111 (1-2), 4–21.

Baker, A.R., Croot, P.L., 2010. Atmospheric and marine controls on aerosol iron solubility in seawater. Mar. Chem. 120, 4–13.

Barbeau, K., Rue, E.L., Bruland, K.W., Butler, A., 2001. Photochemical cycling of iron in the surface ocean mediated by microbial iron(III)-binding ligands. Nature 413 (6854), 409–413.

Boye, M., Van den Berg, C.M.G., de Jong, J.T.M., Leach, H., Croot, P., De Baar, H.J.W., 2001. Organic complexation of iron in the Southern Ocean. Deep-Sea Res. I 48 (6), 1477–1497.

Buma, A.G.J., De Baar, H.J.W., Nolting, R.F., Vanbennekom, A.J., 1991. Metal enrichment experiments in the Weddell-Scotia Seas—effects of iron and manganese on various plankton communities. Limnol. Oceanogr. 36 (8), 1865–1878.

Butler, A., 2005. Marine siderophores and microbial iron mobilization. BioMetals 18 (4), 369–374, http://dx.doi.org/:10.1007/s10534-005-3711-0.

Calace, N., Castrovinci, D., Maresca, V., Petronio, B.M., Pietroletti, M., Scardala, S., 2001. Aquatic humic substances in pack ice-seawater-sediment system. Int. J. Environ. Anal. Chem. 79 (4), 315–329.

Coale, K.H., Johnson, K.S., Fitzwater, S.E., Gordon, R.M., Tanner, S., Chavez, F.P., Ferioli, L., Sakamoto, C., Rogers, P., Millero, F., Steinberg, P., Nightingale, P.,

Cooper, A., Cochlan, W.P., Landry, M.R., Constantinou, J., Rollwagen, G., Trasvina, A., Kudela, R., 1996. A massive phytoplankton bloom induced by an ecosystem-scale iron fertilization experiment in the equatorial Pacific Ocean. Nature 383 (6600), 495–501.

Croot, P.L., Johansson, M., 2000. Determination of iron speciation by cathodic stripping voltammetry in seawater using the competing ligand 2-(2-Thiazolylazo)-p-cresol (TAC). Electroanalysis 12 (8), 565–576.

Croot, P.L., Streu, P., Baker, A.R., 2004. Short residence time for iron in surface seawater impacted by atmospheric dry deposition from Saharan dust events. Geophys. Res. Lett. 31, L23S08.

Croot, P.L., Frew, R.D., Sander, S., Hunter, K.A., Ellwood, M.J., Abraham, E.R., Law, C.S., Smith, M.J., Boyd, P.W., 2007. The effects of physical forcing on iron chemistry and speciation during the Fe Cycle experiment in the South West Pacific. J. Geophys. Res. 112, C06015.

Cullen, J.T., Bergquist, B.A., Moffett, J.W., 2006. Thermodynamic characterization of the partitioning of iron between soluble and colloidal species in the Atlantic Ocean. Mar. Chem. 98 (2–4), 295–303.

Fitzwater, S.E., Johnson, K.S., Gordon, R.M., Coale, K.H., Smith Jr., W.O., 2000. Trace metal concentrations in the Ross Sea and their relationship with nutrients and phytoplankton growth. Deep-Sea Res. II 47 (15–16), 3159–3179.

Gerringa, L.J.A., Herman, P.M.J., Poortvliet, T.C.W., 1995. Comparison of the linear van den Berg/Ružić transformation and a non-linear fit of the Langmuir isotherm applied to Cu speciation data in the estuarine environment. Mar. Chem. 48 (2), 131–142.

Gerringa, L.J.A., Veldhuis, M.J.W., Timmermans, K.R., Sarthou, G., de Baar, H.J.W., 2006. Co-variance of dissolved Fe-binding ligands with biological observations in the Canary Basin. Mar. Chem. 102, 276–290.

Gerringa, L.J.A., Blain, S., Laan, P., Sarthou, G., Veldhuis, M.J.W., Brussaard, C.P.D., Viollier, E., Timmermans, K.R., 2008. Fe-binding organic ligands near the Kerguelen Archipelago in the Southern Ocean (Indian sector). Deep-Sea Res. II 55, 606–621.

Gerringa, L.J.A., Alderkamp, A.-C., Laan, P., Thuróczy, C.-E., De Baar, H.J.W., Mills, M.M., Van Dijken, G.L., Van Haren, H., Arrigo, K.R., 2012. Iron from melting glaciers fuels the phytoplankton blooms in Amundsen Sea (Southern Ocean): iron biogeochemistry. Deep-Sea Res. II 71–76, 16–31.

Gledhill, M., Van Den Berg, C.M.G., 1994. Determination of complexation of iron (III) with natural organic complexing ligands in sea water using cathodic stripping voltammetry. Mar. Chem. 47 (1), 41–54.

Giulivi, C.F., Jacobs, S.S., 1997. Oceanographic data in the Amundsen and Bellingshausen Seas: N.B. Palmer cruise 9402, February—March 1994. Lamont–Doherty Earth Observatory Technical Report 97–3, pp. 330.

Hassler, C.S., Alasonati, E., Mancuso Nichols, C.A., Slaveykova, V.I., 2011a. Exopolysaccharides produced by bacteria isolated from the pelagic Southern Ocean—role in Fe binding, chemical reactivity, and bioavailability. Mar. Chem. 123 (1-4), 88–98.

Hassler, C.S., Schoemann, V., Nichols, C.M., Butler, E.C.V., Boyd, P.W., 2011b. Saccharides enhance iron bioavailability to Southern Ocean phytoplankton. Proc. Natl. Acad. Sci. 108 (3), 1076–1081.

Hudson, R.J.M., Rue, R.L., Bruland, K.W., 2003. Modeling complexometric titrations of natural water samples. Environ. Sci. Technol. 37 (8) 1553–1562, http://dx.doi.org/101021/ES025751A.

Jacobs, S.S., Hellmer, H.H., 1996. Antarctic ice sheet melting in the Southeast Pacific. Geophys. Res. Lett. 23 (9), 957–960.

Jacobs, S.S., Jenkins, A., Giulivi, C.F., Dutrieux, P., 2011. Stronger ocean circulation and increased melting under Pine Island Glacier ice shelf. Nat. Geosci. 4, 519–523.

Jenkins, A., Dutrieux, P., Jacobs, S.S., McPhail, S.D., Perrett, J.R., Webb, A.T., White, D., 2010. Observations beneath Pine Island Glacier in West Antarctica and implications for its retreat. Nat. Geosci. 3 (7), 468–472.

Johnson, K.S., Boyle, E., Bruland, K., Measures, C., Moffett, J., Aquilarislas, A., Barbeau, K., Cai, Y., Chase, Z., Cullen, J., Doi, T., Elrod, V., Fitzwater, S., Gordon, M., King, A., Laan, P., Laglera-Baquer, L., Landing, W., Lohan, M., Mendez, J., Milne, A., Obata, H., Ossiander, L., Plant, J., Sarthou, G., Sedwick, P., Smith, G.J., Sohst, B., Tanner, S., Van Den Berg, S., Wu, J., 2007. Developing standards for dissolved iron in seawater. Eos Trans. AGU 88 (11), 131.

de Jong, J.T.M., den Das, J., Bathmann, U., Stoll, M.H.C., Kattner, G., Nolting, R.F., De Baar, H.J.W., 1998. Dissolved iron at subnanomolar levels in the Southern Ocean as determined by ship-board analysis. Anal. Chim. Acta 377 (2–3), 113–124.

Kepkay, P.E., 1994. Particle aggregation and the biological reactivity of colloids. Mar. Ecol. Prog. Ser. 109 (2-3), 293–304.

Klunder, M.B., Laan, P., Middag, R., De Baar, H.J.W., VanOoijen, J., 2011. Dissolved Fe in the Southern Ocean (Atlantic sector). Deep-Sea Res. II 58, 2678–2694.

Klunder, M.,. De Baar, H.J.W. submitted. Dissolved iron concentrations around the Antarctic Circumpolar Current, Weddell Gyre and Ross Gyre: a compilation, submitted for publication.

Kuma, K., Nakabayashi, S., Suzuki, Y., Kudo, I., Matsunaga, K., 1992. Photoreduction of Fe(III) by dissolved organic substances and existence of Fe(II) in seawater during spring blooms. Mar. Chem. 37, 15–27.

Kuma, K., Nakabayashi, S., Matsunaga, K., 1995. Photoreduction of Fe(III) by hydroxycarboxylic acids in seawater. Water Res. 29, 1559–1569.

Kuma, K., Nishioka, J., Matsunaga, K., 1996. Controls on iron(III) hydroxide solubility in seawater: the influence of pH and natural organic chelators. Limnol. Oceanogr. 41 (3), 396–407.

Lannuzel, D., Schoemann, V., de Jong, J., Tison, J.L., Chou, L., 2007. Distribution and biogeochemical behaviour of iron in the East Antarctic sea ice. Mar. Chem. 106 (1-2), 18–32.

Lannuzel, D., Schoemann, V., de Jong, J., Chou, L., Delille, B., Becquevort, S., Tison, J.L., 2008. Iron study during a time series in the western Weddell pack ice. Mar. Chem. 108 (1-2), 85–95.

Lannuzel, D., Schoemann, V., de Jong, Pasquer, B., Vander Merwe, P., Masson, F., Tison, J.-L., Bowie, A., 2010. Distribution of dissolved iron in Antarctic sea ice: spatial, seasonal, and inter-annual variability. J. Geophys. Res. 115, G03022.

Maldonado, M.T., Strzepek, R.F., Sander, S., Boyd, P.W., 2005. Acquisition of iron bound to strong organic complexes, with different Fe-binding groups and photochemical reactivities, by plankton communities in Fe-limited subantarctic waters. Global Biogeochem. Cycles 19 (4), GB4S23.

Martin, J.H., Gordon, R.M., Fitzwater, S.E., 1990. Iron in Antarctic waters. Nature 345 (6271), 156–158.

Martin, J.H., Gordon, R.M., Fitzwater, S.E., 1991. The case for iron. Limnol. Oceanogr. 36 (8), 1793–1802.

Middag, R., De Baar, H.J.W., Laan, P., Baker, K., 2009. Dissolved aluminium and the silicon cycle in the Arctic Ocean. Mar. Chem. 115 (3–4), 176–195.

Mills, M., Alderkamp, A.-C., Thurcózy, C.-E., van Dijken, G.L., Laan, P., de Baar, H.J.W., Arrigo, K.R., 2012. Phytoplankton biomass and pigment responses to Fe amendments in the Pine Island and Amundsen polynyas. Deep-Sea Res. II 71–76, 61–76.

Nichols, C.M., Bowman, J.P., Guezennec, J., 2005. Effects of incubation temperature on growth and production of exopolysaccharides by an Antarctic sea ice bacterium grown in batch culture. Appl. Environ. Microbiol. 71 (7), 3519–3523.

Nishioka, J., Takeda, S., 2000. Change in the concentrations of iron in different size fractions during growth of the oceanic diatom *Chaetoceros* sp.: importance of small colloidal iron. Mar. Biol. 137 (2), 231–238.

Nishioka, J., Takeda, S., Wong, C.S., Johnson, W.K., 2001. Sized-fractionated iron concentrations in the northeast Pacific Ocean: distribution of soluble and small colloidal iron. Mar. Chem. 74 (2–3), 157–179.

Nistche, F.O., Jacobs, S.S., Larter, R.D., Gohl, K., 2007. Bathymetry of the Amundsen Sea continental shelf: implications for geology, oceanography, and glaciology. Geochem. Geophys. Geosyst. 8, Q10009.

Pankowski, A., McMinn, A., 2008. Ferredoxin and flavodoxin in eastern Antarctica pack ice. Polar Biol. 31 (10), 1153–1165.

Powell, R.T., Wilson-Finelli, A., 2003. Photochemical degradation of organic iron compelxing ligands in seawater. Aquat. Sci. 65, 367–374.

Pusceddu, A., Cattaneo-Vietti, R., Albertelli, G., Fabiano, M., 1999. Origin, biochemical composition and vertical flux of particulate organic matter under the pack ice in Terra Nova Bay (Ross Sea, Antarctica) during late summer 1995. Polar Biol. 22 (2), 124–132.

Raiswell, R., 2011. Iceberg-hosted nanoparticulate Fe in the Southern Ocean: mineralogy, origin, dissolution kinetics and source of bioavailable Fe. Deep-Sea Res. II 58 (11–12), 1364–1375.

Raiswell, R., Tranter, M., Benning, L.G., Siegert, M., De'ath, R., Huybrechts, P., Payne, T., 2006. Contributions from glacially derived sediment to the global iron (oxyhydr)oxide cycle: Implications for iron delivery to the oceans. Geochim. Cosmochim. Acta 70 (11), 2765.

Reimnitz, E., Clayton, J.R., Kempema, E.W., Payne, J.R., Weber, W.S., 1993. Interaction of rising frazil with suspended particles: tank experiments with applications to nature. Cold Regions Sci. Technol. 21 (2), 117–135.

Rignot, E., Bamber, J.L., Van Den Broek, M.R., Davis, C., Li, Y.H., Van De Berg, W.J., Van Meijgaard, E., 2008. Recent Antarctic ice mass loss from radar interferometry and regional climate modelling. Nat. Geosci. 1 (2), 106–110.

Rue, E.L., Bruland, K.W., 1997. The role of organic complexation on ambient iron chemistry in the equatorial Pacific Ocean and the response of a mesoscale iron addition experiment. Limnol. Oceanogr. 42 (5), 901–910.

Sarthou, G., Vincent, D., Christaki, U., Obernosterer, I., Timmermans, K.R., Brussard, C.P.D., 2008. The fate of biogenic iron during a phytoplankton bloom induced by natural fertilisation: impact of copepod grazing. Deep-Sea Res. II 55 (5–7), 734–751.

Sedwick, P.N., DiTullio, G.R., Mackey, D.J., 2000. Iron and manganese in the Ross Sea, Antarctica: seasonal iron limitation in Antarctic shelf waters. J. Geophys. Res. 105 (C5). 11 321-11 336.

Sherwood, C.R., 2000. Numerical model of frazil ice and suspended sediment concentrations and formation of sediment laden ice in the Kara Sea. J. Geophys. Res. 105 (C6), 14061–14080.

Smedsrud, L.H., 1998. Estimating aggregation between suspended sediments and Frazil ice. Geophys. Res. Lett. 25 (20), 3875–3878.

Sunda, W.G., Huntsman, S.A., 1997. Interrelated influence of iron, light and cell size on marine phytoplankton growth. Nature 390 (6658), 389–392.

Thuróczy, C.-E., Boye, B., Losno, R., 2010a. Dissolution of cobalt and zinc from natural and anthropogenic dusts in seawater. Biogeosciences 7 (6), 1927–1936.

Thuróczy, C.-E., Gerringa, L.J.A., Klunder, M.B., Middag, R., Laan, P., Timmermans, K.R., De Baar, H.J.W., 2010b. Speciation of Fe in the Eastern North Atlantic Ocean. Deep-Sea Res. I 57 (11), 1444–1453.

Thuróczy, C.-E., Gerringa, L.J.A., Klunder, M.B., Laan, P., De Baar, H.J.W., 2011a. Observation of consistent trends in the organic complexation of iron in the Atlantic sector of the Southern Ocean. Deep-Sea Res. II 58, 2695–2706, http://dx.doi.org/:10.1016/j.dsr2.2011.01.002.

Thuróczy, C.-E., Gerringa, L.J.A., Klunder, M.B., Laan, P., Le Guitton, M., de Baar, H.J.W., 2011b. Distinct trends in the speciation of iron between the shallow

shelf seas and the deep basins of the Arctic Ocean. J. Geophys. Res. 116, C10009http://dx.doi.org/:10.1029/2010JC006835.
Timmermans, K.R., Davey, M.S., Vander Wagt, B., Snoek, J., Geider, R.J., Veldhuis, M.J.W., Gerringa, L.J.A., De Baar, H.J.W., 2001. Co-limitation by iron and light of *Chaetoceros brevis*, *C. dichaeta* and *C. calcitrans* Bacillariophyceae. Mar. Ecol. Prog. Ser. 217, 287–297.
Turoczy, N.J., Sherwood, J.E., 1997. Modification of the Van den Berg/Ruzic method for the investigation of complexation parameters of natural waters. Anal. Chim. Acta 354 (1–3), 15–21.
Thomas, D.N., Kennedy, H., Kattner, G., Gerdes, D., Gough, C., Dieckmann, G.S., 2001. Biogeochemistry of platelet ice: its influence on particle flux under fast ice in the Weddell Sea, Antarctica. Polar Biol. 24 (7), 486–496.